

# Synthesis and Characterization of $\text{RuH}_2(\text{H}_2)_2(\text{P}^i\text{Pr}_3)_2$ and Related Chemistry. Evidence for a Bis(dihydrogen) Structure

Kamaluddin Abdur-Rashid, Dmitry G. Gusev, Alan J. Lough, and Robert H. Morris\*

Department of Chemistry, University of Toronto, 80 St. George Street, Toronto, Ontario M5S 3H6, Canada

Received August 20, 1999

The complex  $\text{RuH}_2(\text{H}_2)_2(\text{P}^i\text{Pr}_3)_2$  (**1**) was prepared by the protonation of  $[\text{K}(18\text{-crown-6})][\text{RuH}_5(\text{P}^i\text{Pr}_3)_2]$  with 1,3-benzenedimethanol. The observation of H–H and M–H vibrations, short  $T_1(\text{min})$  values of the hydride resonance, the octahedral geometry of the disordered single-crystal X-ray structure of **1**, and large averaged H–D coupling constants for  $\text{RuH}_x\text{D}_{6-x}(\text{P}^i\text{Pr}_3)_2$  provide evidence for two dihydrogen and two hydride ligands. Under an atmosphere of  $\text{N}_2$ , complex **1** readily forms an equilibrium mixture of the dinitrogen complexes  $\text{RuH}_2(\text{N}_2)_2(\text{P}^i\text{Pr}_3)_2$  (**2**) and  $\{\text{RuH}_2(\text{N}_2)(\text{P}^i\text{Pr}_3)_2\}_2(\mu\text{-N}_2)$  (**3**), which readily reverts to **1** under an atmosphere of  $\text{H}_2$ . Slow evaporation of a pentane solution of **1** under an atmosphere of  $\text{N}_2$  gas resulted in the isolation of colorless crystals of **3**. Complex **1** is very unstable with respect to loss of  $\text{H}_2$  and forms the trihydride-bridged classical polyhydride dimer  $(\text{P}^i\text{Pr}_3)_2(\text{H})\text{Ru}(\mu\text{-H})_3\text{Ru}(\text{H})_2(\text{P}^i\text{Pr}_3)_2$  (**4**) under an argon atmosphere or under vacuum at room temperature. Exposure of a solution of **4** to  $\text{H}_2$  gas results in the gradual regeneration of **1**. Similarly, the known bis(dihydrogen) complex  $\text{RuH}_2(\text{H}_2)_2(\text{PCy}_3)_2$  (**5**) was also prepared by protonation of  $[\text{K}(18\text{-crown-6})][\text{RuH}_5(\text{PCy}_3)_2]$ . An attempt to isolate  $\text{RuH}_2(\text{H}_2)_2(\text{PPh}_3)_2$  (**6**) by protonation of  $\text{K}[\text{RuH}_5(\text{PPh}_3)_2]$  resulted in the in situ formation of an equilibrium mixture of the bis(dihydrogen) complex **6** and the nonclassical dimer  $(\text{PPh}_3)_2(\text{H})\text{Ru}(\mu\text{-H})_3\text{Ru}(\text{H})_2(\text{PPh}_3)_2$  (**7**). The crystal structures of **3**, **4**, and **7** are reported.

## Introduction

Only a few bis(dihydrogen) complexes have been reported in the literature,<sup>1–15</sup> since the first such complex,  $[\text{IrH}_2(\text{H}_2)_2(\text{PCy}_3)_2]^+$ , was identified in solution by Crabtree and Lavin.<sup>1</sup> Most of these complexes are inherently unstable and reactive, and their characterization is mainly based on in situ spectroscopic data in

solution<sup>1,13</sup> or in noble-gas matrices.<sup>2,3</sup> To date, only  $\text{RuH}_2(\text{H}_2)_2(\text{PCy}_3)_2$ ,<sup>4–8,11,12</sup>  $\text{Tp}^*\text{RuH}(\text{H}_2)_2$ , and  $\text{Tp}'\text{RuH}(\text{H}_2)_2$  ( $\text{Tp}^* = \text{hydridotris}(3,5\text{-dimethylpyrazolyl})\text{borate}$  and  $\text{Tp}' = \text{hydridotris}(3\text{-isopropyl-4-bromopyrazolyl})\text{borate}$ )<sup>9,10,16</sup> have been isolated as solids. These three complexes possess short  $T_1(\text{min})$  values of 20–35 ms at 300 MHz, indicative of the presence of at least one coordinated dihydrogen ligand, while  $\text{Tp}^*\text{RuH}(\text{H}_2)_2$  and  $\text{Tp}'\text{RuH}(\text{H}_2)_2$  show the characteristic  $\nu_{\text{H-H}}$  band in their infrared spectra at 2361 and 2250  $\text{cm}^{-1}$ , respectively. The large averaged H–D coupling constants of 5.2–5.4 Hz in the partially deuterated derivatives of these two complexes provide evidence for the presence of two coordinated dihydrogen ligands. Rapid hydrogen atom movement between the Ru–dihydrogen (or Ru–HD or Ru–D<sub>2</sub>) and Ru–hydride (or Ru–D) sites precludes the observation of the full  $^1J(\text{HD})$  coupling, which is expected to be about 27 Hz. The assignment of  $\text{RuH}_2(\text{H}_2)_2(\text{PCy}_3)_2$  as a bis(dihydrogen) complex is less definitive because no  $\nu_{\text{H-H}}$  band was observed in the infrared spectrum, no crystal structure has been reported to date, and no H–D couplings were detected in its partially deuterated derivative. However, the very rich reaction chemistry exhibited by this complex<sup>4–8,11,12,16</sup> and its characteristic inelastic neutron scattering spectrum<sup>11</sup> is logically consistent with the presence of two dihydrogen ligands.

- (1) Crabtree, R. H.; Lavin, M. *J. Chem. Soc., Chem. Commun.* **1985**, 1661–1662.
- (2) Sweany, R. L. *J. Am. Chem. Soc.* **1985**, *107*, 2374–2379.
- (3) Upmacis, R. K.; Poliakov, M.; Turner, J. J. *J. Am. Chem. Soc.* **1986**, *108*, 3645–3651.
- (4) Arliguie, T.; Chaudret, B.; Morris, R. H.; Sella, A. *Inorg. Chem.* **1988**, *27*, 598–599.
- (5) Borowski, A. F.; Sabo-Etienne, S.; Christ, M. L.; Donnadieu, B.; Chaudret, B. *Organometallics* **1996**, *15*, 1427–1434.
- (6) Chaudret, B.; Dagnac, P.; Labroue, D.; Sabo-Etienne, S. *New J. Chem.* **1996**, *20*, 1137–1141.
- (7) Christ, M. L.; Sabo-Etienne, S.; Chung, G.; Chaudret, B. *Inorg. Chem.* **1994**, *33*, 5316–5319.
- (8) Christ, M. L.; Sabo-Etienne, S.; Chaudret, B. *Organometallics* **1995**, *14*, 1082–1084.
- (9) Moreno, B.; Sabo-Etienne, S.; Chaudret, B.; Rodriguez-Fernandez, A.; Jalon, F.; Trofimenko, S. *J. Am. Chem. Soc.* **1994**, *116*, 2635–2636.
- (10) Moreno, B.; Sabo-Etienne, S.; Chaudret, B.; Rodriguez, A.; Jalon, F.; Trofimenko, S. *J. Am. Chem. Soc.* **1995**, *117*, 7441–7451.
- (11) Rodriguez, V.; Sabo-Etienne, S.; Chaudret, B.; Thoburn, J.; Ulrich, S.; Limbach, H. H.; Eckert, J.; Barthelat, J. C.; Hussein, K.; Marsden, C. J. *Inorg. Chem.* **1998**, *37*, 3475–3485.
- (12) Sabo-Etienne, S.; Hernandez, M.; Chung, G.; Chaudret, B. *New J. Chem.* **1994**, *18*, 175–177.
- (13) Smith, K. T.; Tilset, M.; Kuhlman, R.; Caulton, K. G. *J. Am. Chem. Soc.* **1995**, *117*, 9473–9480.
- (14) Pacchioni, G. *J. Am. Chem. Soc.* **1990**, *112*, 80–85.
- (15) Dapprich, S.; Frenking, G. *Z. Anorg. Allg. Chem.* **1998**, *624*, 583–589.

- (16) Sabo-Etienne, S.; Chaudret, B. *Coord. Chem. Rev.* **1998**, *180*, 381–407.

Various attempts have also been made to isolate the analogous triisopropylphosphine complex  $\text{RuH}_2(\text{H}_2)_2(\text{P}^i\text{Pr}_3)_2$ , but these have all failed due to its instability, particularly with respect to loss of  $\text{H}_2$ .<sup>17,18</sup> In general, except for  $\text{RuH}_2(\text{H}_2)_2(\text{PCy}_3)_2$ , this reaction has prevented the isolation and characterization of other bis(dihydrogen) species of general formula  $\text{RuH}_2(\text{H}_2)_2(\text{PR}_3)_2$ . Loss of  $\text{H}_2$  from  $\text{RuH}_2(\text{H}_2)_2(\text{PR}_3)_2$  normally results in mixed-valence dimeric species of general formula  $\text{Ru}_2\text{H}_6(\text{PR}_3)_4$ .<sup>16,18,19</sup> To date, no X-ray structures have been reported for these species and both classical and non-classical structures have been assigned on the basis of the analysis of their spectroscopic characteristics.<sup>4,17,18</sup>

Recently, we have reported a high-yielding synthetic method for the preparation of various anionic hydride complexes,<sup>20</sup> including the novel salt  $[\text{K}(18\text{-crown-6})][\text{RuH}_5(\text{P}^i\text{Pr}_3)_2]$ .<sup>21</sup> Protonation of this ruthenium(IV) pentahydride salt with 1,3-benzenedimethanol generates  $\text{RuH}_2(\text{H}_2)_2(\text{P}^i\text{Pr}_3)_2$ . We hereby report the synthesis, isolation, and characterization of this very reactive and unstable complex. This report also demonstrates that the dimeric species  $\text{Ru}_2\text{H}_6(\text{PR}_3)_4$  reversibly regenerates the bis(dihydrogen) species  $\text{RuH}_2(\text{H}_2)_2(\text{PR}_3)_2$  under  $\text{H}_2$ .

Since the reactivity pattern of  $\text{RuH}_2(\text{H}_2)_2(\text{P}^i\text{Pr}_3)_2$  is expected to be similar to that of the analogous tricyclohexylphosphine compound, we have also undertaken an analysis of the reaction of the  $\text{P}^i\text{Pr}_3$  complex with  $\text{N}_2$ . The single-crystal X-ray structure of the novel dinitrogen-bridged tris(dinitrogen) product  $\{\text{RuH}_2(\text{N}_2)(\text{P}^i\text{Pr}_3)_2\}_2(\mu\text{-N}_2)$  is also reported. In addition, we have also demonstrated that our synthetic procedure for  $\text{RuH}_2(\text{H}_2)_2(\text{P}^i\text{Pr}_3)_2$ , which involves the protonation of the anionic hydride conjugate base,<sup>21</sup> provides a convenient and high-yielding route for the preparation of analogous bis(dihydrogen) complexes, including  $\text{RuH}_2(\text{H}_2)_2(\text{PCy}_3)_2$ .

## Experimental Section

**General Considerations.** All preparations and manipulations were carried out under purified  $\text{H}_2$ ,  $\text{N}_2$ , or Ar atmospheres with the use of standard Schlenk, vacuum line, and glovebox techniques in dry, oxygen-free solvents. Tetrahydrofuran (THF), diethyl ether, and hexanes were dried and distilled from sodium benzophenone ketyl. Deuterated solvents were degassed and dried over molecular sieves. Triisopropylphosphine was supplied by Organometallics Inc.  $\text{RuCl}_3 \cdot x\text{H}_2\text{O}$  was obtained as a loan from Johnson Matthey Inc. NMR spectra were recorded on a Varian Unity 500 (500 MHz for  $^1\text{H}$ , 76.7 MHz for  $^2\text{H}$ ) or on a Varian Gemini 300 MHz spectrometer (300 MHz for  $^1\text{H}$  and 121.5 for  $^{31}\text{P}$ ). All  $^{31}\text{P}$  spectra were recorded with proton decoupling, and  $^{31}\text{P}$  chemical shifts were measured relative to 85%  $\text{H}_3\text{PO}_4$  as an external reference.  $^1\text{H}$  chemical shifts were measured relative to partially deuterated solvent peaks but are reported relative to tetramethylsilane.  $^2\text{H}$  chemical shifts were referenced to natural abundance deuterated solvent peaks.  $T_1$  measurements were made at 500 MHz using the inversion recovery method. The temperature of the probe was calibrated using the temperature dependence of the chemical shifts of MeOH. Infrared spectra were obtained

on a Nicolet 550 Magna-IR spectrometer. The ruthenium(IV) salts  $[\text{K}(18\text{-crown-6})][\text{RuH}_5(\text{P}^i\text{Pr}_3)_2]$  and  $[\text{K}][\text{RuH}_5(\text{PPh}_3)_2]$  were prepared according to previously reported procedures.<sup>21,22</sup> We were not able to obtain elemental analyses on the unstable complexes of this work.

**Syntheses.  $\text{RuH}_2(\text{H}_2)_2(\text{P}^i\text{Pr}_3)_2$  (1).** A solution of 1,3-benzenedimethanol (180 mg, 1.3 mmol) in THF (2 mL) was added to a solution of  $[\text{K}(18\text{-crown-6})][\text{RuH}_5(\text{P}^i\text{Pr}_3)_2]$  (900 mg, 1.2 mmol) in THF (5 mL) and stirred for 30 min. The mixture was then filtered and the filtrate evaporated with a stream of  $\text{H}_2$  gas, resulting in an oily residue which was then extracted with pentane (3 mL). The pentane extract was then filtered and the solvent evaporated with a stream of  $\text{H}_2$  gas, resulting in a spectroscopically pure sample of **1** as an oil. Yield: 405 mg (77%).  $^1\text{H}$  NMR (THF- $d_8$ ):  $\delta$  -8.31 (t,  $^2J(\text{HP}) = 8.0$  Hz, 6H, RuH), 1.13 (m, 36H,  $\text{CH}_3$ ), 1.87 (m, 6H, CH).  $^{31}\text{P}\{^1\text{H}\}$  NMR:  $\delta$  88.4 (s). IR (Nujol):  $\nu(\text{H-H})$  2586  $\text{cm}^{-1}$  (br);  $\nu(\text{Ru-H})$  1946, 1930  $\text{cm}^{-1}$  (sh);  $\nu_a(\text{Ru-H}_2)$  1673  $\text{cm}^{-1}$ ;  $\nu_s(\text{Ru-H}_2)$  or  $\delta(\text{Ru-H})$  822  $\text{cm}^{-1}$ .  $^1\text{H}$   $T_1$  (THF- $d_8$ , 500 MHz; ms)/ $T$  (K): 326/294, 263/273, 191/252, 146/231, 119/210, 87/189, 74/178, 63/168, 60/157.  $^1\text{H}$   $T_1$  (toluene- $d_8$ , 300 MHz; ms)/ $T$  (K): 406/293, 113/2233, 72/213, 58/203, 45/193, 45/183; the sample froze at 173 K. Deuteration of  $\text{RuH}_2(\text{H}_2)_2(\text{P}^i\text{Pr}_3)_2$  was accomplished using the following method. A 10 mg sample of **1** dissolved in  $\text{C}_6\text{D}_6$  (0.65 g) was injected into a NMR tube under an argon atmosphere. The tube was then fitted with an adapter equipped with a Teflon stopcock, and this was attached to a vacuum line. The sample was cooled to liquid-nitrogen temperature and degassed under vacuum, and the tube was then closed. When the contents of the tube reached room temperature,  $\text{D}_2$  gas (1 atm) was back-filled into the tube, which was then closed, cooled to liquid-nitrogen temperature, and flame-sealed. The  $^1\text{H}$  NMR spectrum (500 MHz, 293 K) was acquired as soon as the sample attained room temperature and shows the presence of the  $\text{RuHD}_5\text{L}_2$ ,  $\text{RuH}_2\text{D}_4\text{L}_2$ , and  $\text{RuH}_3\text{D}_3\text{L}_2$  isotopomers, with chemical shifts at -8.091, -8.051, and -8.025 ppm, respectively.

**$\{\text{RuH}_2(\text{N}_2)(\text{P}^i\text{Pr}_3)_2\}_2(\mu\text{-N}_2)$  (3).** A solution of 1,3-benzenedimethanol (20 mg, 0.15 mmol) in THF (0.5 mL) was added to a solution of  $[\text{K}(18\text{-crown-6})][\text{RuH}_5(\text{P}^i\text{Pr}_3)_2]$  (100 mg, 0.14 mmol) in THF (0.5 mL), and the mixture was stirred for 30 min under a nitrogen atmosphere. This mixture was then filtered, and the filtrate was evaporated with a stream of  $\text{N}_2$  gas, resulting in a tarry residue which was then extracted with pentane (1 mL). The pentane extract was then filtered and the solvent evaporated with a stream of  $\text{N}_2$  gas, resulting in a tan powder. Yield: 62 mg (97%).  $^1\text{H}$  NMR ( $\text{C}_6\text{D}_6$ ):  $\delta$  -13.3 (broad, 4H, RuH), 1.24 (m, 72H,  $\text{CH}_3$ ), 2.10 (m, 12H, CH).  $^{31}\text{P}\{^1\text{H}\}$  NMR:  $\delta$  70.2 (s, broad). IR (Nujol):  $\nu(\text{N-N})$  2165, 2131, 2141 (sh), 2088  $\text{cm}^{-1}$  (weak);  $\nu(\text{Ru-H})$  1948  $\text{cm}^{-1}$ . IR (THF):  $\nu(\text{N-N})$  2125, 2163, 2061  $\text{cm}^{-1}$  (weak);  $\nu(\text{Ru-H})$  1908  $\text{cm}^{-1}$ . The product was difficult to purify due to its high solubility in various solvents, although a few crystals of  $\{\text{RuH}_2(\text{N}_2)(\text{P}^i\text{Pr}_3)_2\}_2(\mu\text{-N}_2)$  were obtained for an X-ray study (see below). In solution the complex is in equilibrium with the monomeric species  $\text{RuH}_2(\text{N}_2)_2(\text{P}^i\text{Pr}_3)_2$  (**2**). The product also develops a red color under reduced pressure, due to the formation of unstable species that could not be isolated or characterized.

**$(\text{P}^i\text{Pr}_3)_2(\text{H})\text{Ru}(\mu\text{-H})_3\text{Ru}(\text{H})_2(\text{P}^i\text{Pr}_3)_2$  (4).** A solution of  $\text{RuH}_2(\text{H}_2)_2(\text{P}^i\text{Pr}_3)_2$  (20 mg) in hexanes (0.5 mL) was slowly evaporated to dryness under vacuum. The residue was then kept under vacuum for 5 h, quantitatively yielding **4**<sup>18</sup> as a dark red solid.  $^1\text{H}$  NMR (300 MHz, 298 K, THF- $d_8$ ):  $\delta$  -12.9 (broad, 6H, RuH), 1.27 (m, 72H,  $\text{CH}_3$ ), 1.89 (m, 12H, CH).  $^{31}\text{P}\{^1\text{H}\}$  NMR:  $\delta$  90.4 (s, broad). IR (Nujol):  $\nu(\text{Ru-H})$  2032, 1964, 1910, 1580  $\text{cm}^{-1}$ .

**$\text{RuH}_2(\text{H}_2)_2(\text{PCy}_3)_2$  (5).** THF (5.0 mL) was added to  $\text{RuCl}_3 \cdot x\text{H}_2\text{O}$  (150 mg, 0.72 mmol) and tricyclohexylphosphine (410

(17) Chaudret, B.; Devillers, J.; Poilblanc, R. *Organometallics* **1985**, *4*, 1727-1732.

(18) Burrow, T.; Sabo-Etienne, S.; Chaudret, B. *Inorg. Chem.* **1995**, *34*, 2470-2472.

(19) Chaudret, B.; Poilblanc, R. *Organometallics* **1985**, *4*, 1722-1726.

(20) Gusev, D. G.; Lough, A. J.; Morris, R. H. *J. Am. Chem. Soc.* **1998**, *120*, 13138-13147.

(21) Abdur-Rashid, K.; Gusev, D. G.; Lough, A. J.; Morris, R. H. *Organometallics* **2000**, *19*, 834-843.

(22) Wilczynski, R.; Fordyce, W. A.; Halpern, J. *J. Am. Chem. Soc.* **1983**, *105*, 2066-2068.

**Table 1. Summary of Crystal Data, Details of Intensity Collection, and Least-Squares Refinement Parameters for 1, 3, 4, and 7**

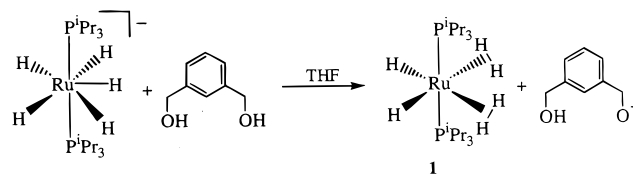
	1	3	4	7
empirical formula	C <sub>18</sub> H <sub>18</sub> P <sub>2</sub> Ru	C <sub>36</sub> H <sub>88</sub> N <sub>6</sub> P <sub>4</sub> Ru <sub>2</sub>	C <sub>36</sub> H <sub>90</sub> P <sub>4</sub> Ru <sub>2</sub>	C <sub>76</sub> H <sub>73</sub> OP <sub>4</sub> Ru <sub>2</sub>
<i>M<sub>r</sub></i>	427.57	931.14	849.10	1328.36
cryst size, mm	0.25 × 0.24 × 0.23	0.30 × 0.28 × 0.31	0.38 × 0.34 × 0.28	0.15 × 0.15 × 0.20
cryst class	triclinic	monoclinic	orthorhombic	monoclinic
space group	<i>P</i> $\bar{1}$	<i>P</i> 2 <sub>1</sub> / <i>c</i>	<i>Pbca</i>	<i>P</i> 2 <sub>1</sub> / <i>n</i>
temp, K	100	150	100	100
<i>a</i> , Å	7.9310(9)	15.377(1)	21.7419(3)	14.7037(3)
<i>b</i> , Å	7.9684(6)	18.4860(1)	16.3501(4)	20.7219(7)
<i>c</i> , Å	9.1903(9)	17.4630(1)	24.7136(5)	21.3139(6)
$\alpha$ , deg	99.361(6)	90	90	90
$\beta$ , deg	90.170(4)	106.799(1)	90	96.224(2)
$\gamma$ , deg	99.550(6)	90	90	90
<i>V</i> , Å <sup>3</sup>	564.86(9)	4752.2(5)	8785.2(3)	6455.8(3)
<i>Z</i>	1	4	8	4
<i>D</i> <sub>calcd</sub> , g cm <sup>-3</sup>	1.257	1.301	1.284	1.367
$\mu$ (Mo K $\alpha$ ), mm <sup>-1</sup>	0.832	0.800	0.855	0.612
<i>F</i> (000)	230	1976	3632	2740
$\theta$ range collected, deg	4.25–25.01	1.38–26.35	4.10–28.27	4.10–25.01
no. of rflns	2376	18 146	40 694	43 796
no. of indep rflns	1942	9324	10 826	11 312
<i>R</i> 1 [ <i>I</i> > 2 $\sigma$ ( <i>I</i> )] <sup>a</sup>	0.0364	0.0209	0.0391	0.0450
w <i>R</i> 2 (all data) <sup>a</sup>	0.0822	0.0716	0.0936	0.1064
goodness of fit	0.969	1.071	1.024	1.000
no. of params refined	110	473	427	768
max peak in final $\Delta F$ map, e Å <sup>-3</sup>	0.316	0.432	1.395	0.971

<sup>a</sup> Definition of *R* indices: *R*1 =  $\sum(F_o - F_c)/\sum(F_o)$ ; w*R*2 =  $[\sum[w(F_o^2 - F_c^2)^2]/\sum[w(F_o^2)^2]]^{1/2}$ .

mg, 1.46 mmol), and the resulting mixture was refluxed for 3 h under an argon atmosphere. The solvent was then removed under vacuum, and KH (250 mg, 6.25 mmol) and 18-crown-6 (190 mg, 0.72 mmol) were added. THF (5.0 mL) was then injected into the flask under a flow of H<sub>2</sub> gas, and the mixture was stirred for 2 h, after which it was filtered and the solids were washed with THF and then hexanes and dried in vacuo. The insoluble residue (mixture of [K(18-crown-6)][RuH<sub>5</sub>(PCy<sub>3</sub>)<sub>2</sub>], KCl, and excess KH) was transferred to a 50 mL Schlenk flask and 10 mL of THF added. The mixture was cooled to -80 °C and 2-propanol (1.0 mL) added dropwise under a flow of hydrogen, with constant and vigorous stirring (*Caution!*). The mixture was then slowly warmed to room temperature and stirred for another 1 h. The solvent was evaporated under a stream of H<sub>2</sub> gas and the resulting residue cooled to -80 °C. Water (5.0 mL) was added, and the mixture was slowly warmed to room temperature. It was filtered, and the solids were washed with water (2 × 1.0 mL) and then methanol (2 × 1.0 mL) and dried in a stream of H<sub>2</sub> gas. Yield: 268 mg (56%). The <sup>1</sup>H and <sup>31</sup>P NMR and IR spectra correspond to those reported in the literature for RuH<sub>2</sub>(H<sub>2</sub>)<sub>2</sub>(PCy<sub>3</sub>)<sub>2</sub>.<sup>4</sup>

**RuH<sub>2</sub>(H<sub>2</sub>)<sub>2</sub>(PPh<sub>3</sub>)<sub>2</sub> (6).** A solution of 1,3-benzenedimethanol (12.5 mg, 0.07 mmol) in THF (2 mL) was added to a solution of K[RuH<sub>5</sub>(PPh<sub>3</sub>)<sub>2</sub>] (60 mg, 0.09 mmol) in THF (5 mL), and this mixture was stirred for 4 h under H<sub>2</sub>. The mixture was then filtered and the filtrate evaporated with a stream of H<sub>2</sub> gas. The resulting solids were then extracted with C<sub>6</sub>D<sub>6</sub> and transferred to an NMR tube, which was then sealed under H<sub>2</sub> (1 atm). The <sup>1</sup>H and <sup>31</sup>P{<sup>1</sup>H} NMR spectra show the presence of an approximately equimolar mixture of **6** and (PPh<sub>3</sub>)<sub>2</sub>(H)Ru( $\mu$ -H)<sub>3</sub>Ru(H<sub>2</sub>)(PPh<sub>3</sub>)<sub>2</sub> (**7**).<sup>17</sup>

**X-ray Structure Analysis.** Colorless crystals of **1** emerged from the isolated oil after standing for 5 days at room temperature at a pressure of 3.5 atm of H<sub>2</sub>. Crystals of **3** and **4** were obtained from the slow evaporation of pentane solutions of the respective complexes. Crystals of **7**, as Ru<sub>2</sub>H<sub>6</sub>(PPh<sub>3</sub>)<sub>4</sub>·THF, were obtained by layering a THF solution of freshly prepared **6** (containing approximately 50% **7**) with pentane. Data for **1**, **4**, and **7** were collected on a Nonius Kappa-CCD diffractometer and for **3** on a Siemens P4 diffractometer using Mo K $\alpha$  radiation ( $\lambda$  = 0.710 73 Å). The CCD data were integrated and scaled using the DENZO-SMN software package, and the structures were solved and refined using SHELX-

**Scheme 1**

TL version 5.0. The hydrides in **3**, **4**, and **7** were located and refined isotropically. A common isotropic thermal parameter was determined for the two hydrogen atoms of the dihydrogen ligand in **7**; hence, these were refined with geometric constraints (H(5RU)–H(6RU) = 1.00 ± 0.01 Å). The crystallographic data for **1**, **3**, **4**, and **7** are summarized in Table 1.

## Results and Discussion

**Synthesis and Characterization of RuH<sub>2</sub>(H<sub>2</sub>)<sub>2</sub>-(P<sup>i</sup>Pr<sub>3</sub>)<sub>2</sub>.** Protonation of [K(18-crown-6)][RuH<sub>5</sub>(P<sup>i</sup>Pr<sub>3</sub>)<sub>2</sub>] by 1,3-benzenedimethanol in THF results in the nearly quantitative formation of the neutral bis(dihydrogen) complex RuH<sub>2</sub>(H<sub>2</sub>)<sub>2</sub>(P<sup>i</sup>Pr<sub>3</sub>)<sub>2</sub> (**1**), while the sparingly soluble [K(18-crown-6)][C<sub>6</sub>H<sub>4</sub>(CH<sub>2</sub>OH)(CH<sub>2</sub>O)] precipitated and was removed by filtration (Scheme 1). Workup yielded **1** as an oil from which colorless crystals gradually emerged after standing under an H<sub>2</sub> atmosphere. Complex **1** is extremely air sensitive and is very soluble in most common solvents. It must be stored under H<sub>2</sub> gas at -30 °C in its pure state or as a solution in hexane or THF because it readily loses H<sub>2</sub> to form a red dimer and readily reacts with N<sub>2</sub> to form an equilibrium mixture of dinitrogen complexes (see below).

Figure 1 shows the structure of **1** as found in a unit cell of the crystal at 100 K. The phosphine ligands are trans, and the ruthenium atom is located at an inversion center. The four peaks located in the final difference map (Figure 1b) (including those from crystallographic symmetry), which represent approximately 1.5 electrons each, are interpreted as the electron density peaks of



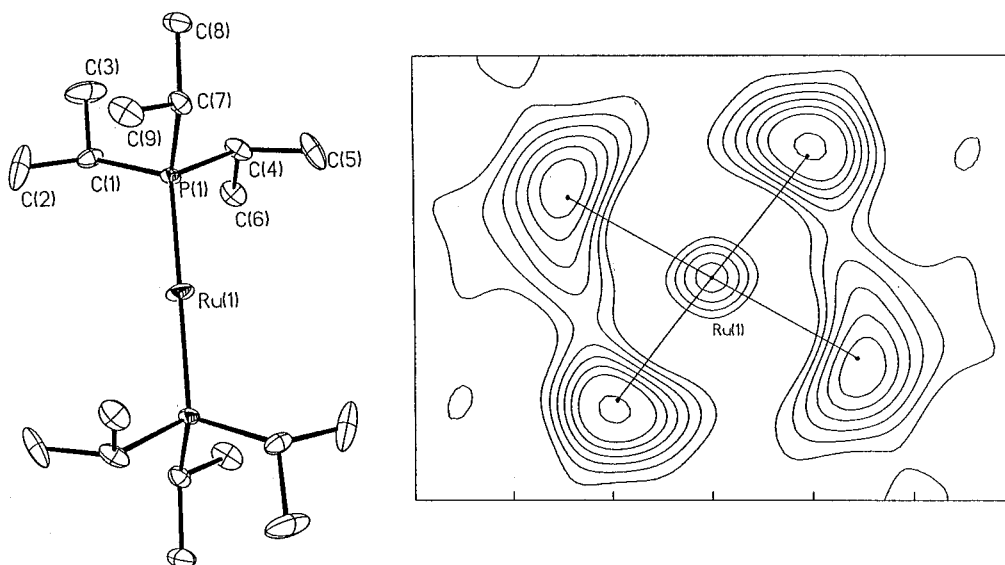


**Figure 1.** (a, left) Molecular structure and atomic numbering of  $\text{RuH}_2(\text{H}_2)_2(\text{P}^i\text{Pr}_3)_2$  (**1**). (b, right) Final difference Fourier map calculated through the equatorial plane of the molecule, in which the contributions from the H and  $\text{H}_2$  ligands were not included. Contours are at the  $1 \text{ e } \text{\AA}^{-3}$  level.  $\text{Ru}(1)-\text{P}(1) = 2.3163(7) \text{ \AA}$ ;  $\text{P}(1)\#1-\text{Ru}(1)-\text{P}(1) = 180.00(3)^\circ$ .

two H ligands and two  $\text{H}_2$  ligands that are disordered about the inversion center. The distances of the peak maxima are 1.61 and 1.75  $\text{\AA}$  from the ruthenium atom.

The octahedral coordination mode of the complex is consistent with a bis(dihydrogen) dihydride structure. Both cis and trans geometries of the hydride and dihydrogen ligands might be possible. The  $180^\circ$  P–Ru–P angle is more consistent with a disordered trans structure, since the *cis*-dihydride was calculated to have a P–Ru–P angle of  $163.8^\circ$ .<sup>11</sup> However, these calculations also showed that the trans isomer is expected to be approximately 5–12  $\text{kcal mol}^{-1}$  (depending on the method) less stable than the cis isomer. A center of symmetry would also be observed in the cis isomer if there were either a dynamic or a static disorder in the structure. A static disorder would be the result of a 4-fold disorder of the two  $\text{H}_2$  and two H<sup>−</sup> ligands, while a dynamic disorder would be the consequence of the “cis effect”<sup>23</sup> due to interaction of the hydrides with the neighboring dihydrogens, allowing easy exchange of the H atoms. The unusually large and flattened oblate shape of the thermal displacement of the ruthenium atom relative to the phosphorus atoms is indicative of disorder within the symmetry plane of the molecule.

The infrared spectrum (Nujol) of the complex (Figure 2) shows a broad and strong H–H mode at  $2586 \text{ cm}^{-1}$  and a weak, broad M– $\text{H}_2$  mode at  $1673 \text{ cm}^{-1}$ . There is also a very intense and broad Ru–H band at  $1946 \text{ cm}^{-1}$  with a shoulder at  $1930 \text{ cm}^{-1}$ .<sup>24</sup> These bands were absent in the infrared spectrum of the hexadeuteride analogue,  $\text{RuD}_2(\text{D}_2)_2(\text{P}^i\text{Pr}_3)_2$ , which was generated by stirring a hexane solution of **1** under an atmosphere of  $\text{D}_2$  gas (1 atm). The deuteration studies also revealed an intense M–H/M– $\text{H}_2$  band at  $822 \text{ cm}^{-1}$  for **1**.

The solution NMR spectra of **1** are consistent with previous in situ spectroscopic data for the complex.<sup>18</sup> The  $^1\text{H}$  NMR spectrum in  $\text{THF}-d_8$  shows a single triplet

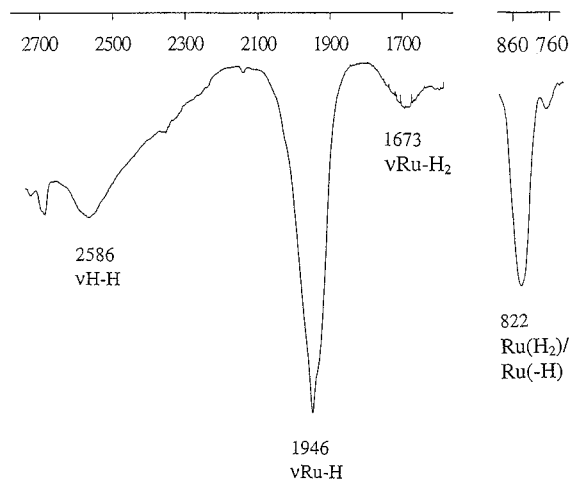


**Figure 2.** Infrared spectrum (Nujol mull) of  $\text{RuH}_2(\text{H}_2)_2(\text{P}^i\text{Pr}_3)_2$ .

at  $-8.31 \text{ ppm}$  ( $^2J_{\text{HP}} = 8.0 \text{ Hz}$ ) for both the hydrogen and hydride ligands, while a singlet at  $88.4 \text{ ppm}$  is observed in the  $^{31}\text{P}\{^1\text{H}\}$  NMR, indicating that the two phosphine ligands are equivalent.

The hydrides of **1** readily exchange with  $\text{D}_2$  gas at room temperature. Thus, when a solution of the complex in  $\text{C}_6\text{D}_6$  was sealed under  $\text{D}_2$  gas (1 atm), the  $^1\text{H}$  (300 MHz) NMR spectrum showed a decrease in the hydride resonance by 95% within 10 min. The  $^1\text{H}$  NMR spectrum in the high-field region (Figure 3a) reveals the presence of the  $\text{RuHD}_5\text{L}_2$  and  $\text{RuH}_2\text{D}_4\text{L}_2$  isotopomers ( $\text{RuD}_6\text{L}_2$  is also present), each with the H and D sites in fast exchange. A sample that is more enriched in hydrogen produces resonances in a 500 MHz  $^1\text{H}$  NMR spectrum for the  $\text{RuH}_3\text{D}_3\text{L}_2$  isotopomers as well as the other two (Figure 3b). The spectra show line splittings due to HD ( $4.0 \pm 0.1 \text{ Hz}$ ) and HP (8.0 Hz) couplings. The  $^1\text{H}^2\text{D}_5^3\text{P}_2$ ,  $^1\text{H}_2^2\text{D}_4^3\text{P}_2$ , and  $^1\text{H}_3^2\text{D}_3^3\text{P}_2$  spin systems, with equivalent D due to exchange and equivalent P nuclei due to symmetry, produce 15, 13, and 11 lines in the  $^1\text{H}$  spectra, respectively, because  $J_{\text{HP}}$  is a multiple of  $J_{\text{HD}}^{\text{av}}$ . The simulations suggest that there is an isotopic perturbation of the exchange-averaged proton shift to

(23) Van Der Sluys, L. S.; Eckert, J.; Eisenstein, O.; Hall, J. H.; Huffman, J. C.; Jackson, S. A.; Koetzle, T. F.; Kubas, G. J.; Vergamini, P. J.; Caulton, K. G. *J. Am. Chem. Soc.* **1990**, *112*, 4831–4841.

(24) Bender, B. R.; Kubas, G. J.; Jones, L. H.; Swanson, B. I.; Eckert, J.; Capps, K. B.; Hoff, C. D. *J. Am. Chem. Soc.* **1997**, *119*, 9179–9190.

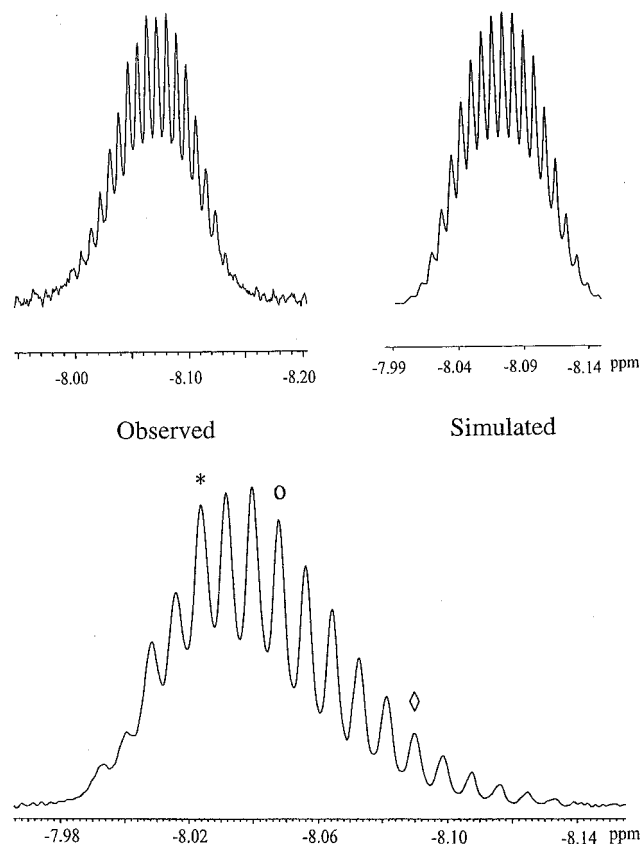


**Figure 3.** (a, top) Observed and simulated  $^1\text{H}$  NMR spectra at 500 MHz in the hydride region of the mixture of isotopomers  $\text{RuHD}_5(\text{P}^i\text{Pr}_3)_2$  and  $\text{RuH}_2\text{D}_4(\text{P}^i\text{Pr}_3)_2$  in  $\text{C}_6\text{D}_6$  in the mole fraction ratio 0.84:0.16 and with chemical shifts of  $-8.091$  and  $-8.051$  ppm, respectively. (b, bottom)  $^1\text{H}$  NMR spectrum at 500 MHz of the mixture of isotopomers  $\text{RuHD}_5\text{L}_2$  ( $\diamond$ )  $\text{RuH}_2\text{D}_4\text{L}_2$  ( $\circ$ ) and  $\text{RuH}_3\text{D}_3\text{L}_2$  ( $*$ ) with mole fractions 0.40, 0.42, and 0.18, respectively. The chemical shifts and  $T_2$  values are respectively  $-8.091$ ,  $-8.051$ , and  $-8.025$  ppm and 0.14, 0.11, and 0.09 s. In all spectra  $J_{\text{HD}}^{\text{av}} = 4.0$  Hz and  $J_{\text{HP}} = 8.0$  Hz.

lower field when each deuterium is replaced by hydrogen. Consistent with this, the lines become broader and  $T_2$  times shorter as each deuterium is replaced by hydrogen.  $T_1$  measurements of the lines of the spectrum in Figure 3b revealed a decrease with increasing chemical shift as expected. The chemical shifts of the isotopomers  $^1\text{H}_4^2\text{D}_2^3\text{P}_2$  and  $^1\text{H}_5^2\text{D}^3\text{P}_2$  were not determined.

Since the H–H stretching frequency is greater than that of the Ru–H, a slight excess of deuterium is expected in the nonclassical sites. This is consistent with the observation that the chemical shift of the  $\text{H}_2\text{D}_4$  isotopomer is 0.040 ppm downfield of the  $\text{HD}_5$  isotopomer, assuming typical values of, for example,  $\delta(\text{H}_2) = \delta(\text{HD}) \cong -6.6$  and  $\delta(\text{H}) \cong -11$  ppm with  $[\text{Ru}(\text{D})_2(\text{HD})(\text{D}_2)(\text{P}^i\text{Pr}_3)_2]/[\text{Ru}(\text{H})(\text{D})(\text{D}_2)(\text{P}^i\text{Pr}_3)_2] \cong 0.98$ . The trend of upfield shift of the averaged  $^1\text{H}$  chemical shift of the hydride/dihydrogen resonance when H is replaced by D is also observed for the bis(dihydrogen) complexes  $\text{Ru}(\text{H}_2)_2\text{H}(\text{HB}(\text{pz}-3,5\text{-Me})_3)$  and  $\text{Ru}(\text{H}_2)_2\text{H}(\text{HB}(\text{pz}-3\text{-}^i\text{Pr}-4\text{-Br})_3)$ .<sup>10</sup> Both upfield and downfield shifts on replacement of hydride for deuteride have been reported for classical and nonclassical polyhydrides, and the origins for these shifts are usually not clear (see the references in Oldham et al.<sup>25</sup>).

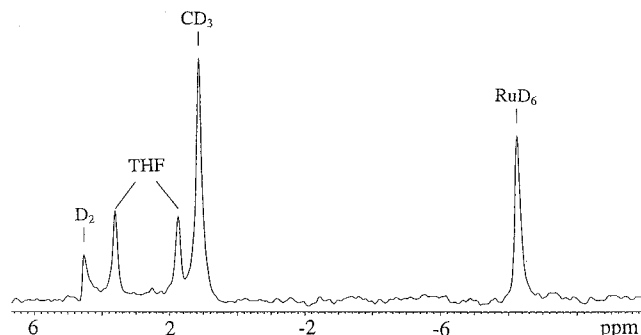


**Figure 4.**  $^2\text{H}$  NMR spectrum of  $\text{RuH}_2(\text{H}_2)_2(\text{P}^i\text{Pr}_3)_2$  at 500 MHz in THF under  $\text{D}_2$  gas (1 atm).

With the assumption of  $^2J_{\text{HD}} \cong 2 \pm 2$  Hz for a hydride–deuteride coupling ( $\text{Ru}(\text{H})(\text{D})$ ), a  $^1J_{\text{HD}}$  value of  $30 \pm 1$  Hz is obtained for the  $\text{Ru}(\text{D})_2(\text{HD})(\text{D}_2)(\text{P}^i\text{Pr}_3)_2/\text{Ru}(\text{H})(\text{D})(\text{D}_2)_2(\text{P}^i\text{Pr}_3)_2$  formulation with  $J_{\text{HD}}^{\text{av}}$  of 4.0 Hz. This  $^1J_{\text{HD}}$  value corresponds to an H–H distance in the dihydrogen ligand of 0.92 Å.<sup>26</sup> On the other hand, if the mono(dihydrogen) formulation  $\text{Ru}(\text{D})_4(\text{HD})(\text{P}^i\text{Pr}_3)_2/\text{Ru}(\text{H})(\text{D})_3(\text{D}_2)(\text{P}^i\text{Pr}_3)_2$  is assumed instead, an impossibly large  $^1J_{\text{HD}}$  value of 58 Hz is calculated, which is larger than the 43.2 Hz for free HD.<sup>10,13</sup>

A  $^2\text{H}$  NMR spectrum of **1** under  $\text{D}_2$  gas (1 atm) in THF at 20 °C (Figure 4) indicates that the hydride hydrogens and the methyl protons of the phosphine ligands readily undergo H/D exchange, whereas no deuterium incorporation is observed for the methine protons. The mechanism for this exchange process probably involves the intermediacy of the 16-electron species  $\text{RuH}_2(\text{H}_2)(\text{P}^i\text{Pr}_3)_2$ . Coordination of an isopropylphosphine methyl as an agostic C–H could eventually result in catalytic deuteration of the methyl protons, either by an oxidative addition or direct hydrogen/deuterium atom exchange mechanism. The infrared spectrum (Nujol) of **1** under argon shows a band at 2711  $\text{cm}^{-1}$ , which may be due to the  $\nu(\text{CH}-\text{M})$  band of an agostic C–H bond in  $\text{RuH}_2(\text{H}_2)(\text{P}^i\text{Pr}_3)_2$ .<sup>27</sup>

The  $T_1$  value of the hydrogen ligands of **1** in  $\text{THF}-d_8$  approaches a minimum value of about 60 ms at 500 MHz. A  $T_1$  value of 52 ms is calculated<sup>28</sup> using the crystallographic structural parameters for **1** with two “fast-spinning”<sup>29</sup> cis or trans dihydrogen ligands with H–H distances of 0.94 Å. Therefore, all the data are consistent with a bis(dihydrogen) formulation in the solid state and in solution.

**Synthesis and Structure of  $\{\text{RuH}_2(\text{N}_2)(\text{P}^i\text{Pr}_3)_2\}_2(\mu\text{-N}_2)$ .** Complex **1**, in its pure state or in solution, reacts readily with dinitrogen. Evaporation of a pentane solution of the product resulted in the isolation of the thermally stable dinitrogen-bridged tris(dinitrogen) complex **3**, which readily reverts to **1** under an atmosphere of  $\text{H}_2$ . The room-temperature  $^1\text{H}$  NMR spectrum shows a single broad resonance at  $-13.3$  ppm, which is due to

(25) Oldham, W. J.; Hinkle, A. S.; Heinekey, D. M. *J. Am. Chem. Soc.* **1997**, *119*, 11028–11036.

(26) Maltby, P. A.; Steinbeck, M.; Lough, A. J.; Morris, R. H.; Klooster, W. T.; Koetzle, T. F.; Srivastava, R. C. *J. Am. Chem. Soc.* **1996**, *118*, 5396–5407.

(27) Crabtree, R. H.; Hamilton, D. G. *Adv. Organomet. Chem.* **1988**, *28*, 299–338.

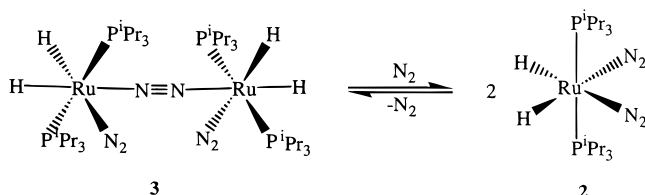
(28) Desrosiers, P. J.; Cai, L.; Lin, Z.; Richards, R.; Halpern, J. *J. Am. Chem. Soc.* **1991**, *113*, 4173–4184.

(29) Earl, K. A.; Jia, G.; Maltby, P. A.; Morris, R. H. *J. Am. Chem. Soc.* **1991**, *113*, 3027–3039.

**Table 2.** Selected Bond Lengths and Angles around Ru(1) of **3** and Equivalent Parameters<sup>a</sup> around Ru(2)<sup>a</sup>

Bond Distances (Å)			
Ru(1)–H(1RU)	1.57(2), 1.59(2)*	Ru(1)–H(2RU)	1.60(2), 1.62(2)*
Ru(1)–N(1)	2.051(1), 2.049(1)*	Ru(1)–N(3)	2.017(2), 2.009(2)*
Ru(1)–P(1)	2.3372(5), 2.3373(5)*	Ru(1)–P(2)	2.3313(5), 2.3330(5)*
N(1)–N(2)	1.113(2), 1.113(2)*	N(3)–N(4)	1.105(2), 1.107(2)*
Bond Angles (deg)			
H(1RU)–Ru(1)–N(3)	94.8(6), 92.9(6)*	H(2RU)–Ru(1)–N(3)	176.3(6), 176.5(6)*
H(1RU)–Ru(1)–N(1)	172.6(6), 174.1(6)*	H(2RU)–Ru(1)–N(1)	91.0(6), 88.9(6)*
H(1RU)–Ru(1)–P(2)	79.6(6), 82.6(6)*	H(2RU)–Ru(1)–P(2)	82.9(6), 83.9(6)*
H(1RU)–Ru(1)–H(2RU)	83.7(9), 85.3(9)*	P(2)–Ru(1)–P(1)	155.57(2), 162.26(2)*
N(3)–Ru(1)–P(2)	93.47(4), 92.92(4)*	N(3)–Ru(1)–P(1)	100.53(4), 97.63(4)*
N(1)–Ru(1)–P(2)	104.92(4), 97.52(4)*	N(1)–Ru(1)–P(1)	94.86(4), 96.13(4)*
N(3)–Ru(1)–N(1)	90.84(5), 93.00(6)*		

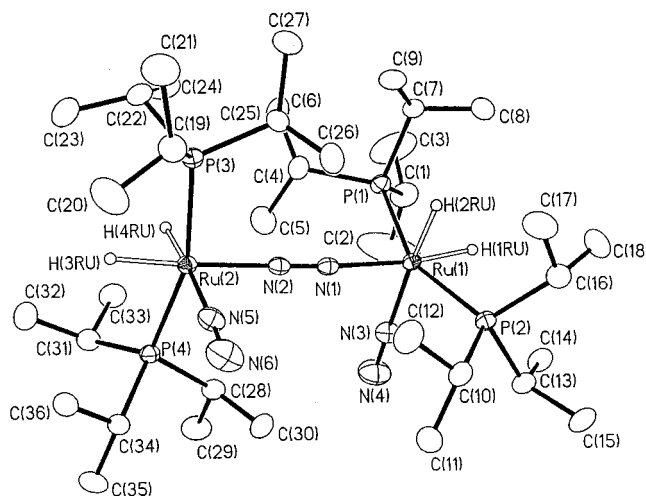
<sup>a</sup> Marked with an asterisk. Although the atoms are not related by crystallographic symmetry, the geometries around Ru(1) and Ru(2) are identical: Ru(1) = Ru(2); N(1) = N(2); N(3) = N(5); P(1) = P(3); P(2) = P(4); H(1RU) = H(3RU); H(2RU) = H(4RU).

**Scheme 2**

the presence of an equilibrium mixture of the dimer **3** and monomeric species,  $\text{RuH}_2(\text{N}_2)_2(\text{P}^i\text{Pr}_3)_2$  (**2**) in rapid exchange (Scheme 2).

The  $^{31}\text{P}$  NMR spectrum shows a broad singlet at 71.6 ppm. Cooling the mixture results in decoalescence, which is complete at 233 K, and clearly shows the presence of the two complexes in the ratio **2**:**3** = 2:1. The  $^1\text{H}$  NMR spectrum at 233 K shows an intense triplet ( $J_{\text{HP}} = 22.2$  Hz) at  $-12.97$  ppm, which is due to the presence of the monomer **2**. This is very similar to the reported  $^1\text{H}$  NMR spectrum of the analogous complex  $\text{RuH}_2(\text{N}_2)_2(\text{PCy}_3)_2$  ( $\delta -12.8$  ppm,  $J_{\text{HP}} = 22$  Hz).<sup>7,12</sup> On the other hand, two distinct hydride chemical shifts were observed for the dimer **3** at  $-13.13$  and  $-14.51$  ppm ( $J_{\text{HP}} = 23.4$  Hz and  $J_{\text{HH}} = 8.1$  Hz). The lowest  $T_1$  value obtained for the hydride resonance is 390 ms (500 MHz) at 193 K (complex **2**), which clearly implies a classical dihydride structure for **2**.<sup>28</sup> The  $^{31}\text{P}\{^1\text{H}\}$  NMR spectrum at 233 K shows two sharp singlets of nearly equal intensity at 73.6 and 76.3 ppm for **2** and **3**.

The solution infrared spectrum (THF) shows two intense  $\nu(\text{N}=\text{N})$  bands at 2163 and 2125  $\text{cm}^{-1}$  and a weak one at 2061  $\text{cm}^{-1}$ , along with a  $\nu(\text{Ru}=\text{H})$  band at 1908  $\text{cm}^{-1}$  (m). The solid-state infrared spectrum (Nujol mull) shows  $\nu(\text{N}=\text{N})$  stretching modes at 2165, 2131, 2141 (sh), and 2088  $\text{cm}^{-1}$  (weak) and the  $\nu(\text{Ru}=\text{H})$  mode at 1948  $\text{cm}^{-1}$ . In comparison, the reported  $\nu(\text{N}=\text{N})$  bands for the solution infrared spectrum of  $\text{RuH}_2(\text{N}_2)_2(\text{PCy}_3)_2$  occur at 2163 and 2126  $\text{cm}^{-1}$ .<sup>7,12</sup> The weak  $\nu(\text{N}=\text{N})$  band at 2061  $\text{cm}^{-1}$  in the solution infrared spectrum of **3** may be due to the vibrational mode of the bridging  $\text{N}_2$  ligand. This mode is normally not observed in the infrared but may be rendered active due to small dipole changes as a result of the nonlinearity of the bridging  $\text{N}_2$  bond or due to coupling to other vibrational modes of the molecule. Steric congestion in the tricyclohexylphosphine complex possibly prevents the formation of a dinitrogen-bridged dimer as observed for the triisopropylphosphine complex; the cone angles of  $\text{PCy}_3$  and  $\text{P}^i\text{Pr}_3$  are 170 and 160°, respectively.<sup>30</sup>

**Figure 5.** Molecular structure and atomic numbering of  $\{\text{RuH}_2(\text{N}_2)(\text{P}^i\text{Pr}_3)_2\}_2(\mu\text{-N}_2)$  (**3**).

The molecular structure of **3** along with the atomic numbering scheme is shown in Figure 5, while selected bond lengths and angles are displayed in Table 2. The structure consists of two identical  $\text{RuH}_2(\text{N}_2)(\text{P}^i\text{Pr}_3)_2$  moieties connected by a bridging dinitrogen ligand, resulting in a distorted-octahedral disposition about each ruthenium center. On each ruthenium atom the phosphine ligands are trans to each other. Two of the hydrides are trans to the terminal  $\text{N}_2$  ligands, while the other two lie along the axis of the molecule. The octahedra are rotated approximately 90° to each other about the Ru–Ru axis so that a terminal  $\text{N}_2$  ligand and the hydride hydrogen trans to it are each eclipsed by the phosphine ligands on the neighboring ruthenium atom. This sterically favorable arrangement could also facilitate the overlap of the two orthogonal  $\pi^*$  orbitals of the  $\mu\text{-N}_2$  ligand with the available  $d\pi$  orbital of each metal. Similar structural dispositions of the  $\text{N}_2$  ligands have been reported for various dinitrogen complexes of tungsten and zirconium.<sup>31,32</sup> The two terminal N–N bond lengths (1.107(2) and 1.105(2) Å) are only slightly longer than in free  $\text{N}_2$  (1.0976 Å) and slightly shorter than the bridging dinitrogen ligand (1.113(2) Å). These bond lengths are also comparable to those reported for terminal and bridging  $\text{N}_2$  ligands in mononuclear

(30) Chen, L.; Poë, A. J. *Coord. Chem. Rev.* **1995**, *143*, 265–295.

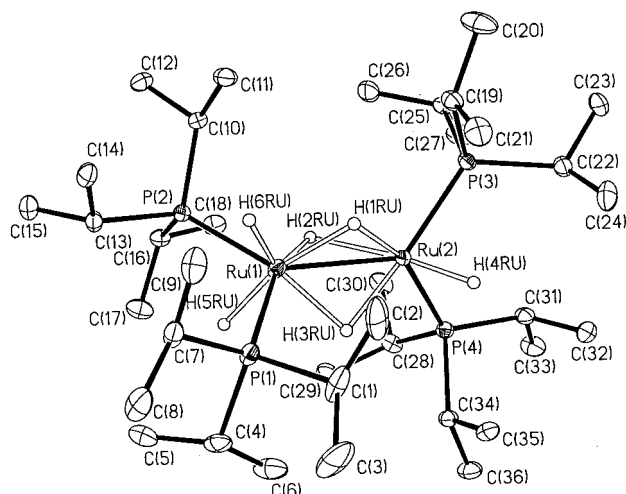
(31) Sanner, R. D.; Manriquez, J. M.; Marsh, R. E.; Bercaw, J. E. *J. Am. Chem. Soc.* **1976**, *98*, 8351–8357.

(32) Anderson, S. N.; Richards, R. L.; Hughes, D. L. *J. Chem. Soc., Dalton Trans.* **1986**, 245–252.



**Table 3.** Selected Bond Lengths and Angles for **4**

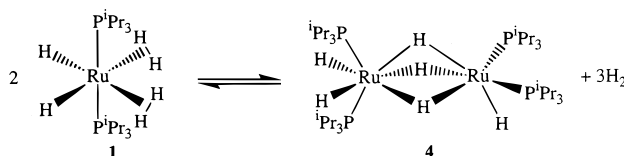
Bond Distances (Å)							
Ru(1)–H(1RU)	1.79(4)	Ru(1)–H(6RU)	1.52(3)	Ru(2)–H(1RU)	1.96(5)	Ru(2)–P(3)	2.2877(7)
Ru(1)–H(2RU)	1.78(4)	Ru(1)–P(2)	2.2820(8)	Ru(2)–H(2RU)	1.97(4)	Ru(2)–P(4)	2.2801(8)
Ru(1)–H(3RU)	1.84(4)	Ru(1)–P(1)	2.3303(8)	Ru(2)–H(3RU)	1.86(4)		
Ru(1)–H(5RU)	1.75(3)	Ru(1)–Ru(2)	2.5889(3)	Ru(2)–H(4RU)	1.66(3)		
Bond Angles (deg)							
P(2)–Ru(1)–P(1)	113.10(3)	P(1)–Ru(1)–Ru(2)	118.45(2)	P(2)–Ru(1)–Ru(2)	128.42(2)		
P(4)–Ru(2)–P(3)	106.75(3)	P(3)–Ru(2)–Ru(1)	126.93(2)	P(4)–Ru(2)–Ru(1)	122.72(2)		
H(6RU)–Ru(1)–H(5RU)	124(2)	H(6RU)–Ru(1)–H(3RU)	142(2)	H(6RU)–Ru(1)–H(2RU)	122(2)		
H(6RU)–Ru(1)–H(1RU)	71(2)	H(5RU)–Ru(1)–H(1RU)	164(2)	H(5RU)–Ru(1)–H(3RU)	84(2)		
H(4RU)–Ru(2)–H(2RU)	165(2)	H(4RU)–Ru(2)–H(1RU)	93(2)	H(4RU)–Ru(2)–H(3RU)	97(2)		
Ru(1)–H(1RU)–Ru(2)	87(2)	Ru(1)–H(2RU)–Ru(2)	87(2)	Ru(1)–H(3RU)–Ru(2)	89(2)		

**Figure 6.** Molecular structure and atomic numbering of  $\text{Ru}_2\text{H}_6(\text{P}^i\text{Pr}_3)_4$  (**4**).

and dinuclear ruthenium(II) complexes.<sup>31</sup> The Ru–N–N bond angles of the two terminal  $\text{N}_2$  (176.0(2) and 176.3(2)°) and the bridging  $\text{N}_2$  (175.2(1) and 179.6(1)°) ligands are similar and show only slight deviation from the expected linear arrangement.

**Formation and Structure of  $(\text{P}^i\text{Pr}_3)_2(\text{H})\text{Ru}(\mu\text{-H})_3\text{Ru}(\text{H})_2(\text{P}^i\text{Pr}_3)_2$ .** Without an  $\text{H}_2$  atmosphere or under vacuum, complex **1** gradually develops a red color due to the formation of the known dimeric species  $(\text{P}^i\text{Pr}_3)_2(\text{H})\text{Ru}(\mu\text{-H})_3\text{Ru}(\text{H})_2(\text{P}^i\text{Pr}_3)_2$  (**4**) as a result of loss of  $\text{H}_2$ .<sup>18</sup> When a THF solution of this dimer was reexposed to  $\text{H}_2$  gas, it gradually reverted to **1**, with 80% conversion after 5 days at 1 atm and 90% after 5 h at 3.5 atm. Thus, **4** can serve as a stable and convenient source of the more reactive and unstable bis(dihydrogen) complex (Scheme 3). There was no evidence of incorporation of  $\text{N}_2$  into **4** even after prolonged exposure of both the solid and a THF solution to  $\text{N}_2$  gas at 3.5 atm. On the other hand, exposure of **4** to  $\text{D}_2$  gas (1 atm) only results in the formation of isotopomers of **1**. These observations, along with the previously reported lowest observed  $T_1$  value of 110 ms (243 K, 250 MHz),<sup>18</sup> suggest the absence of a coordinated dihydrogen ligand in **4**.<sup>33</sup>

Slow evaporation of a pentane solution of **4** results in dark red orthorhombic crystals. Figure 6 shows the molecular structure as determined by the single-crystal X-ray diffraction along with the atomic labeling scheme, while selected bond lengths and angles are listed in Table 3. The structure reveals that **4** is a classical hexahydride dimer with three bridging hydrides. The

**Scheme 3**

Ru–H bond lengths of the terminal hydrides are significantly shorter (1.52(3)–1.75(3) Å) than the bridging ones (1.78(4)–1.97(4) Å). The stereochemistry about Ru(1) is that of a distorted capped octahedron, with the bridging hydrides constituting a common face of this, as well as that of the distorted octahedron about Ru(2). The separation of 2.88 Å between the two terminal hydride hydrogens, H(5RU) and H(6RU), is definitely indicative of a classical structure. The closest approach between two of the hydride hydrogens is 1.94 Å, involving one bridging and one terminal hydride, H(1RU) and H(6RU), respectively.

Our attempt to isolate  $\text{RuH}_2(\text{H}_2)_2(\text{PPh}_3)_2$  (**6**) by protonation of the salt  $\text{K}[\text{RuH}_5(\text{PPh}_3)_2]$  with benzenedimethanol resulted in a mixture of this complex and the dimeric species  $(\text{PPh}_3)_2(\text{H})\text{Ru}(\mu\text{-H})_3\text{Ru}(\text{H}_2)(\text{PPh}_3)_2$  (**7**),<sup>17</sup> both of which were identified by comparison with their previously reported in situ NMR spectra. The latter complex was isolated as bright red monoclinic crystals on layering a THF solution of the mixture with pentane. Exposure of a solution of the dimer in benzene to a  $\text{N}_2$  atmosphere resulted in the quantitative formation of the known complex  $\text{Ru}_2\text{H}_4(\text{N}_2)(\text{PPh}_3)_4$ ,<sup>17</sup> which reverts to the dimer under 1 atm of  $\text{H}_2$ . Complex **7**, unlike **4**, is a nonclassical species, appropriately formulated as  $(\text{PPh}_3)_2(\text{H})\text{Ru}(\mu\text{-H})_3\text{Ru}(\text{H}_2)(\text{PPh}_3)_2$ .<sup>4</sup> This is corroborated by the crystal structure of **7**, which is shown in Figure 7. Selected bond lengths and bond angles for the complex are listed in Table 4.

The complex crystallizes as  $(\text{PPh}_3)_2(\text{H})\text{Ru}(\mu\text{-H})_3\text{Ru}(\text{H}_2)(\text{PPh}_3)_2 \cdot \text{THF}$  with two ruthenium moieties linked together to form a trihydride-bridged face-sharing bioctahedron. Two phosphine ligands are bonded to each ruthenium, with a terminal hydride, H(4RU), completing the octahedron on Ru(1) and an  $\eta^2\text{-H}_2$  (H(5RU) and H(6RU)) ligand on Ru(2). The distance between H(5RU) and H(6RU) in Figure 7 had to be fixed for proper refinement, and so the H–H distance of 1.0 Å is artificial. The terminal hydride and the  $\eta^2\text{-H}_2$  ligands each eclipse a phosphine ligand on the adjacent metal, while the remaining two phosphine ligands are staggered relative to each other. The Ru(1)–Ru(2) distance

(33) Jessop, P. G.; Morris, R. H. *Coord. Chem. Rev.* **1992**, 121, 155–284.

Table 4. Selected Bond Lengths and Angles for 7

Bond Distances (Å)					
Ru(1)–P(1)	2.253(1)	Ru(1)–P(2)	2.226(1)	Ru(2)–P(3)	2.294(1)
Ru(1)–H(1RU)	1.91(4)	Ru(1)–H(2RU)	1.88(4)	Ru(1)–H(3RU)	1.77(4)
Ru(2)–H(1RU)	1.56(5)	Ru(2)–H(2RU)	1.66(4)	Ru(2)–H(3RU)	1.73(3)
Ru(2)–H(6RU)	1.81(3)	H(5RU)–H(6RU)	1.00 <sup>a</sup>	Ru(1)–Ru(2)	2.5523(4)
Bond Angles (deg)					
P(2)–Ru(1)–P(1)	99.17(4)	P(1)–Ru(1)–Ru(2)	130.69(3)	P(2)–Ru(1)–Ru(2)	117.16(3)
P(3)–Ru(2)–P(4)	100.08(4)	P(3)–Ru(2)–Ru(1)	119.06(3)	P(4)–Ru(2)–Ru(1)	125.77(3)
H(4RU)–Ru(1)–H(2RU)	165(2)	H(4RU)–Ru(1)–H(3RU)	96(2)	H(4RU)–Ru(1)–H(1RU)	105(2)
Ru(2)–H(1RU)–Ru(1)	94(2)	Ru(2)–H(2RU)–Ru(1)	92(2)	Ru(2)–H(3RU)–Ru(1)	94(2)
H(1RU)–Ru(2)–H(5RU)	162(2)	H(2RU)–Ru(2)–H(5RU)	82(2)	H(3RU)–Ru(2)–H(5RU)	100(2)
H(1RU)–Ru(2)–H(6RU)	159(2)	H(2RU)–Ru(2)–H(6RU)	104(2)	H(3RU)–Ru(2)–H(6RU)	83(2)

<sup>a</sup> Distance constrained to  $1.00 \pm 0.01$  Å in the refinement.

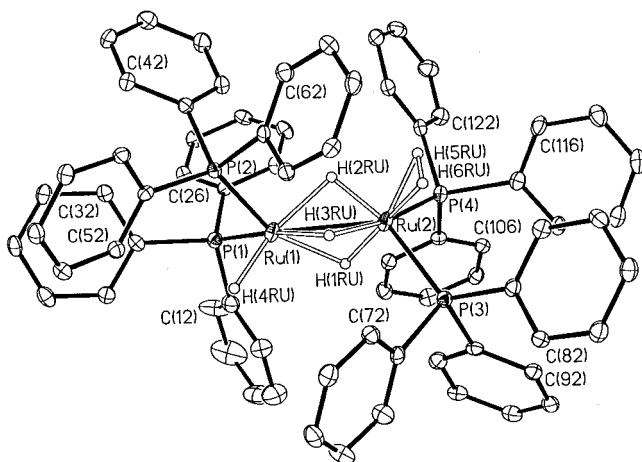


Figure 7. Molecular structure and atomic numbering of  $\text{Ru}_2\text{H}_4(\text{H}_2)(\text{PPh}_3)_4$  (7).

of 2.5523(4) Å is typical for ruthenium and osmium dimers bridged by three hydride ligands.<sup>17,34,35</sup>

Several examples of dimeric ruthenium complexes containing halide and hydridohalide bridges are known.<sup>36–45</sup> However, there are only a few examples of ruthenium dimers in which the bridging ligands are solely hydrides.<sup>17,34,46,47</sup> These include the 32-electron dihydride-bridged cation  $[\text{Ru}_2(\mu\text{-H})_2\text{H}_2(\text{PMe}_3)_6]^+$ , with a Ru–Ru separation of 2.811(1) Å between the ruthenium atoms,<sup>46</sup> and the 30-electron tetrahydride-bridged complex  $\text{Cp}^*\text{Ru}(\mu\text{-H})_4\text{RuCp}^*$ , with a Ru–Ru distance of

2.463(1) Å,<sup>47</sup> which is shorter than the trihydride-bridged Ru–Ru distances in 30-electron complexes **4** (2.5899(3) Å; Table 3) and **7** (2.5523(4) Å; Table 4). Likewise, the metal–metal separation in 30-electron  $\text{Ru}_2(\mu\text{-H}_3)\text{H}(\text{N}_2)(\text{PPh}_3)_4$ , the dinitrogen analogue of **7**, is 2.553(5) Å.<sup>17</sup>

Most of these hydride-bridged ruthenium dimers are characteristically reactive and labile, with  $\text{H}_2$  and other small molecules readily inserting into the M–H bridges to generate monomeric addition products. Likewise, both 30-electron complexes **4** and **7** are readily converted to the respective monomeric bis(dihydrogen) species under a  $\text{H}_2$  atmosphere. In the past the presence of a Ru≡Ru triple bond has been invoked to reconcile the 30-electron count with the 18-electron rule. However, the lability and reactivity of these dimeric species suggest that the three weak three-center–two-electron Ru–H–Ru bonds provide the dominant component of bonding between the two metal atoms in a fashion similar to the B–H–B bonds in 12-electron  $\text{B}_2\text{H}_6$ .

The complex  $\text{Ru}_2\text{H}_6(\text{PCy}_3)_4$  was also prepared from the bis(dihydrogen) complex **5**, using the reported procedure.<sup>4</sup> Exposing a THF solution of this dimer to  $\text{H}_2$  gas resulted in the regeneration of **5**. Interestingly, Arliguie et al.<sup>4</sup> have reported that the dimer has a nonclassical structure similar to that for **7**, rather than the classical structure observed in the solid state for **4**. Normally, it is expected that the greater nucleophilicity of the ruthenium moieties in  $\text{Ru}_2\text{H}_6(\text{PCy}_3)_4$  due to stronger  $\sigma$ -donor  $\text{PCy}_3$  ligands would tend to favor a classical structure. The steric congestion in the molecule is probably a factor favoring the presence of the  $\eta^2\text{-H}_2$  ligand in this complex.

## Conclusion

Protonation of  $[\text{K}(18\text{-crown-6})][\text{RuH}_5(\text{P}^i\text{Pr}_3)_2]$  quantitatively yields the bis(dihydrogen) complex  $\text{RuH}_2(\text{H}_2)_2(\text{P}^i\text{Pr}_3)_2$ , which was isolated for the first time. The presence of the  $\nu(\text{H}–\text{H})$  band in the infrared spectrum, short minimum  $T_1$  value of the hydride resonance, and large averaged H–D coupling constant of  $30 \pm 1$  Hz in the partially deuterated derivative, as well as the octahedral coordination mode of the two phosphine and six hydride ligands in the crystal structure, conclusively suggest the presence of two coordinated dihydrogen ligands. The reaction of  $\text{RuH}_2(\text{H}_2)_2(\text{P}^i\text{Pr}_3)_2$  with  $\text{N}_2$  gas generates the bis(dinitrogen) complex  $\text{RuH}_2(\text{N}_2)_2(\text{P}^i\text{Pr}_3)_2$ , which is in equilibrium with the novel dinitrogen-bridged tris(dinitrogen) complex  $\{\text{RuH}_2(\text{N}_2)(\text{P}^i\text{Pr}_3)_2\}_2(\mu\text{-N}_2)$ . The latter is the first such group 8 metal species to contain both terminal and bridging dinitrogen ligands.

(34) Van Der Sluys, L. S.; Kubas, G. J.; Caulton, K. G. *Organometallics* **1991**, 10, 1033–1038.

(35) Green, M. A.; Huffman, J. C.; Caulton, K. G. *J. Organomet. Chem.* **1983**, 243, C78–C82.

(36) Cotton, F. A.; Torralba, R. C. *Inorg. Chem.* **1991**, 30, 2196–2207.

(37) Chau, D.; James, B. R. *Inorg. Chim. Acta* **1995**, 240, 419–425.

(38) Dekleva, T. W.; Thorburn, I. S.; James, B. R. *Inorg. Chim. Acta* **1985**, 100, 49–56.

(39) Joshi, A. M.; James, B. R. *J. Chem. Soc., Chem. Commun.* **1989**, 1785–1786.

(40) Joshi, A. M.; Macfarlane, K. S.; James, B. R. *J. Organomet. Chem.* **1995**, 488, 161–167.

(41) Hampton, C.; Cullen, W. R.; James, B. R. *J. Am. Chem. Soc.* **1988**, 110, 6918–6919.

(42) Hampton, C.; Dekleva, T. W.; James, B. R.; Cullen, W. R. *Inorg. Chim. Acta* **1988**, 145, 165–166.

(43) Hampton, C. R. S. M.; Butler, I. R.; Cullen, W. R.; James, B. R.; Charland, J. P.; Simpson, J. *Inorg. Chem.* **1992**, 31, 5509–5520.

(44) Macfarlane, K. S.; Joshi, A. M.; Rettig, S. J.; James, B. R. *Chem. Commun.* **1997**, 1363–1364.

(45) Macfarlane, K. S.; Thorburn, I. S.; Cyr, P. W.; Chau, D.; Rettig, S. J.; James, B. R. *Inorg. Chim. Acta* **1998**, 270, 130–144.

(46) Jones, R. A.; Wilkinson, G.; Colquhoun, I. J.; McFarlane, W.; Galas, A. M. R.; Hursthouse, M. B. *J. Chem. Soc., Dalton Trans.* **1980**, 2480–2487.

(47) Suzuki, H.; Omori, H.; Lee, D. H.; Yoshida, Y.; Moro-oka, Y. *Organometallics* **1988**, 7, 2243–2245.



The instability of  $\text{RuH}_2(\text{H}_2)_2(\text{P}^i\text{Pr}_3)_2$  leads to the formation of the known dimer  $(\text{P}^i\text{Pr}_3)_2(\text{H})\text{Ru}(\mu\text{-H})_3\text{Ru}(\text{H})_2(\text{P}^i\text{Pr}_3)_2$ , due to the loss of  $\text{H}_2$ . We have shown that this reaction is reversible; hence, the dimer can be utilized as a thermally stable source of the bis(dihydrogen) complex. Finally, we have demonstrated that our synthetic procedure for  $\text{RuH}_2(\text{H}_2)_2(\text{P}^i\text{Pr}_3)_2$  can also be used for the preparation of analogous bis(dihydrogen) bis(phosphine) species. This is particularly significant, considering that it is now known that these species can be directly used as hydrogenation catalysts,<sup>16,48</sup> as well as for the preparation of ruthenium carbenes  $\text{Ru}(\text{CRR}')\text{-Cl}_2(\text{PR}_3)_2$  that are useful in alkene metathesis methodology.<sup>29,49–53</sup>

(48) Beatty, R. P.; Paciello, R. A. U.S. Patent WO 96/23802-23804, 1996.

**Acknowledgment.** This work was supported by a grant to R.H.M. from the NSERC of Canada and a loan of ruthenium(III) chloride from Johnson Matthey Ltd. Dr. Timothy Burrow is gratefully acknowledged for assistance with the high-field NMR studies.

**Supporting Information Available:** X-ray crystallographic tables for complexes **1**, **3**, **4**, and **7** and  $^1\text{H}$  NMR spectra of **1** and **2/3**. This material is available free of charge via the Internet at <http://pubs.acs.org>.

OM990669I

(49) Nguyen, S. T.; Johnson, L. K.; Grubbs, R. H. *J. Am. Chem. Soc.* **1992**, *114*, 3974–3975.

(50) Olivan, M.; Caulton, K. G. *Chem. Commun.* **1997**, 1733.

(51) Olivan, M.; Clot, E.; Eisenstein, O.; Caulton, K. G. *Organometallics* **1998**, *17*, 3091–3100.

(52) Olivan, M.; Caulton, K. G. *Inorg. Chem.* **1999**, *38*, 566–570.

(53) Wilhelm, T. E.; Belderrain, T. R.; Brown, S. N.; Grubbs, R. H. *Organometallics* **1997**, *16*, 3867–3869.